



(51) International Patent Classification:

H04B 10/70 (2013.01) *G02B 27/28* (2006.01)
B82Y 20/00 (2011.01) *G02F 1/035* (2006.01)
G02B 27/09 (2006.01) *H04B 10/25* (2013.01)

(21) International Application Number:

PCT/CA2021/050686

(22) International Filing Date:

20 May 2021 (20.05.2021)

(25) Filing Language:

English

(26) Publication Language:

English

(30) Priority Data:

63/029,987 26 May 2020 (26.05.2020) US

(71) Applicant: NATIONAL RESEARCH COUNCIL OF CANADA [CA/CA]; 1200 Montreal Road, Building M55, Room C29, Ottawa, Ontario K1A 0R6 (CA).

(72) Inventors: **BOUCHARD, Frédéric**; 79 rue de la Cité-Jardin, Gatineau, Québec J8T 0E5 (CA). **ENGLAND, Duncan**; 25 Columbus Ave., Ottawa, Ontario K1K 1R2 (CA). **BUSTARD, Philip J.**; 83 Vaughan St., Ottawa, Ontario K1M 1X3 (CA). **HESHAMI, Khabat**; 3377 McCarthy Road, Ottawa, Ontario K1V 9G4 (CA). **SUSSMAN, Benjamin**; 423-205 Bolton Street, Ottawa, Ontario K1N 1K7 (CA).

(74) Agent: SABETA, Anton C. et al.; Aird & McBurney LP, 181 Bay Street, Suite 1800, Toronto, Ontario M5J 2T9 (CA).

(81) Designated States (unless otherwise indicated, for every kind of national protection available): AE, AG, AL, AM, AO, AT, AU, AZ, BA, BB, BG, BH, BN, BR, BW, BY, BZ, CA, CH, CL, CN, CO, CR, CU, CZ, DE, DJ, DK, DM, DO, DZ, EC, EE, EG, ES, FI, GB, GD, GE, GH, GM, GT, HN, HR, HU, ID, IL, IN, IR, IS, IT, JO, JP, KE, KG, KH, KN, KP, KR, KW, KZ, LA, LC, LK, LR, LS, LU, LY, MA, MD, ME, MG, MK, MN, MW, MX, MY, MZ, NA, NG, NI, NO, NZ, OM, PA, PE, PG, PH, PL, PT, QA, RO, RS, RU, RW, SA, SC, SD, SE, SG, SK, SL, ST, SV, SY, TH, TJ, TM, TN, TR, TT, TZ, UA, UG, US, UZ, VC, VN, WS, ZA, ZM, ZW.

(84) Designated States (unless otherwise indicated, for every kind of regional protection available): ARIPO (BW, GH, GM, KE, LR, LS, MW, MZ, NA, RW, SD, SL, ST, SZ, TZ, UG, ZM, ZW), Eurasian (AM, AZ, BY, KG, KZ, RU, TJ, TM), European (AL, AT, BE, BG, CH, CY, CZ, DE, DK, EE, ES, FI, FR, GB, GR, HR, HU, IE, IS, IT, LT, LU, LV, MC, MK, MT, NL, NO, PL, PT, RO, RS, SE, SI, SK, SM, TR), OAPI (BF, BJ, CF, CG, CI, CM, GA, GN, GQ, GW, KM, ML, MR, NE, SN, TD, TG).

Declarations under Rule 4.17:

— as to applicant's entitlement to apply for and be granted a patent (Rule 4.17(ii))

(54) Title: ULTRAFAST TEMPORAL FILTERING FOR QUANTUM COMMUNICATIONS

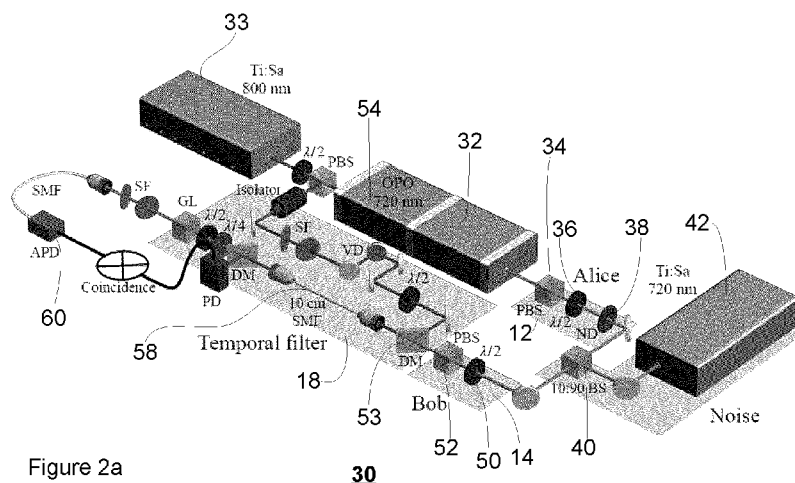


Figure 2a

(57) Abstract: A quantum communication method comprising: at a sender, preparing photons encoded in a single spatial, spectral, and temporal (SST) mode to form a quantum signal; and introducing the quantum signal into a quantum channel; at a receiver, a detector and filtering system optically processing the quantum signal and rejecting background noise photons in the quantum channel, and performing active temporal filtering by switching the polarization of the quantum signal without substantially adding noise; and wherein the active temporal filtering minimizes saturation of the detector.



Published:

- *with international search report (Art. 21(3))*
- *in black and white; the international application as filed contained color or greyscale and is available for download from PATENTSCOPE*

ULTRAFAST TEMPORAL FILTERING FOR QUANTUM COMMUNICATIONS**FIELD**

[0001] Aspects of the disclosure relate to a quantum communication system.

BACKGROUND

[0002] Quantum communication protocols, such as quantum key distribution (QKD), are based on the distribution of entangled photons, or pulses of single photons, throughout an untrusted quantum channel. Quantum key distribution is a technique which results in the sharing of cryptographic keys between two parties: a transmitter often referred to as “Alice”; and a receiver often referred to as “Bob”. In realistic implementations, the quantum channel presents several important challenges such as the presence of loss and noise which degrades the quantum states of the photons propagating through it. For instance, noise ultimately limits the maximal achievable distances and secret key rates in quantum communications. In particular, the operation of quantum communication in extremely noisy environments is becoming even more crucial with the advent of quantum communication with satellites requiring operation in daylight conditions or the development of the quantum internet in existing bright fibre networks.

[0003] Several approaches have been proposed to limit the impact of noise in quantum communications. For example, incremental technological advancements on the single photon source and the single photon detectors have resulted in larger source rates and lower dark count detection rates, which increase the signal-to-noise ratio and minimize the impact of noise. Another approach consists in a change of software by considering quantum protocols that are intrinsically more noise tolerant, e.g. tomographic and high-dimensional protocols. However, a change in quantum protocol typically results in a minor improvement in noise tolerance. Yet another approach involves noise filtering, where spectral, timing and spatial filters may be applied using passive or active schemes.

[0004] At present, the temporal filtering of the quantum signal is limited by the electronics of the single photon detectors. In particular, the jitter of the detectors

dictates the minimal temporal filtering that can be applied to the signal (typically on the order of nanoseconds). In addition, spectral filtering can be employed with a high efficiency using interference filters (typically on the order of nanometers). However, if one were to use Fourier-limited single photon pulses, for a bandwidth of 1 nm, a pulse with a duration of 1 ps can be expected in the near-infrared region.

[0005] Spectral filtering is commonly employed in QKD using interference filters with bandwidths on the order of a few nanometers. Other techniques may achieve narrower bandwidths, but typically presents certain limitations. On the other hand, time filtering can also be jointly employed with the help of fast detectors and time tagging devices, where gating times are limited by the timing jitter of the single photon detectors, typically on the order of nanoseconds, and all other electronic devices involved. With the recent development of superconducting nanowire single photon detectors, a significant improvement in timing jitters can be achieved, i.e. as low as 50 ps. Unfortunately, these detectors require cryogenic cooling (approximately 1 K). Finally, despite time gating being an effective way to limit the amount of noise introduced in the detection event, noise counts may have another undesired effect, i.e. to limit the overall signal detection rate due to detector dead time and detector saturation.

[0006] It is an object of the present disclosure to mitigate or obviate at least one of the above-mentioned disadvantages.

SUMMARY

[0007] In one of its aspects, there is provided a quantum communication method comprising:

at a sender, preparing photons encoded in a single spatial, spectral, and temporal (SST) mode to form a quantum signal; and introducing the quantum signal into a quantum channel;

at a receiver, a detector and filtering system optically processing the quantum signal and rejecting background noise photons in the quantum channel, and performing active temporal filtering by switching the polarization of the quantum

signal without substantially adding noise; and wherein the active temporal filtering minimizes saturation of the detector.

[0008] In another of its aspects, there is provided a quantum communication system comprising:

a sender comprising a quantum signal source and a quantum signal encoder;

a transmission medium;

a receiver comprising an active temporal filter and a single photon detector.

[0009] In another of its aspects, there is provided an active temporal filter comprising:

a system optically processing a quantum signal and rejecting background noise photons in a quantum channel; operating by

a switch comprising a switching efficiency, η , of the quantum signal, wherein the switching efficiency is dependent on at least the nonlinear refractive index of the single mode fibre and the length of the single mode fibre.

[0010] Advantageously, one aspect of the disclosure teaches increasing the overall performance of quantum key distribution in noisy environments by employing a temporal filtering scheme prior to a single photon detector. An ultrafast, active optical switch achieves temporal filtering which allows quantum key distribution in noisy environments by switching the polarization of quantum optical signals without substantially adding noise. The switch matches the shortest possible gate time allowed for quantum signals with a bandwidth on the order of 1 nm. The wavelength of the control and signal pulses is selected in such a way to limit the amount of noise originating from the presence of the strong control-pulse into the spectral window of the signal pulse. In addition, the disclosed technique uses broadband and Fourier-limited quantum signals to maximize spectral and temporal degree of freedom in quantum communication. The technique is compatible with passive spatial and spectral filtering and offers orders of magnitude additional improvement.

BRIEF DESCRIPTION OF THE DRAWINGS

[0011] Several exemplary embodiments of the present disclosure will now be described, by way of example only, with reference to the appended drawings in which:

- [0012] Figure 1a shows a top-level component architecture diagram for a quantum communication system;
- [0013] Figure 1b shows a temporal profile and a spectral profile of a noisy signal;
- [0014] Figure 1c shows a temporal profile and a spectral profile of a noisy signal following temporal filtering;
- [0015] Figure 1d shows a temporal profile and a spectral profile of a noisy signal following active temporal filtering;
- [0016] Figure 1e shows a flowchart outlining exemplary steps for implementing active temporal filtering;
- [0017] Figure 2a shows an experimental setup demonstrating the use of an active temporal filter in the quantum communication system;
- [0018] Figure 2b depicts a temporal profile of the active temporal filter illustrating switching efficiency as a function of the pump delay;
- [0019] Figure 2c show a spectrum of signal photons after spectral filtering at a receiver stage;
- [0020] Figure 3a shows secret key rates as a function of noise counts reported for different channel loss values: 5, 10, 15, and 20 dB;
- [0021] Figure 3b shows a noise threshold for different values of channel loss;
- [0022] Figure 3c shows a noise improvement factor corresponding to the ratio of the noise threshold for the case of active temporal filtering over electronic temporal filtering for different values of channel loss;
- [0023] Figure 3d shows secret rates as a function of channel loss;
- [0024] Figure 3e shows active temporal filtering for different channel noise values, N ;
- [0025] Figure 3f shows loss threshold for different values of noise counts; and
- [0026] Figure 3g shows distance improvement factor corresponding to the ratio of the loss threshold for the case of active temporal filtering over electronic temporal filtering for different values of noise counts.

DETAILED DESCRIPTION OF EXEMPLARY EMBODIMENTS

[0027] The following detailed description refers to the accompanying drawings. Wherever possible, the same reference numbers are used in the drawings and the following description to refer to the same or similar elements. While embodiments of the disclosure may be described, modifications, adaptations, and other implementations are possible. For example, substitutions, additions, or modifications may be made to the elements illustrated in the drawings, and the methods described herein may be modified by substituting, reordering, or adding stages to the disclosed methods. Accordingly, the following detailed description does not limit the disclosure. Instead, the proper scope of the disclosure is defined by the appended claims.

[0028] Moreover, it should be appreciated that the particular implementations shown and described herein are illustrative of the invention and are not intended to otherwise limit the scope of the present invention in any way. Indeed, for the sake of brevity, certain sub-components of the individual operating components, conventional data networking, application development and other functional aspects of the systems may not be described in detail herein. Furthermore, the connecting lines shown in the various figures contained herein are intended to represent exemplary functional relationships and/or physical couplings between the various elements. It should be noted that many alternative or additional functional relationships or physical connections may be present in a practical system.

[0029] Referring to Figure 1a, there is shown a top-level component architecture diagram for a quantum communication system, generally depicted by reference numeral 10. Quantum communication system 10 comprises sender 12 which transmits information to receiver 14 by encoded single quanta, such as single photons via quantum channel 16. Generally, each photon carries one bit of information encoded upon a property of the photon, such as its polarization, phase or energy/time. The photon may even carry more than one bit of information, for example, by using properties such as angular momentum. Quantum channel 16 may be a communication link between transmitter 12 and receiver 14, and quantum channel 16 may be in the

form of an optical fibre link, underwater links, free space, air, or any combination thereof.

[0030] Sender 12 comprises suitable light source and encoder; and receiver 14 comprises quantum receiver with one or more detectors configured to detect quantum signals. Positioned before receiver 14 is active temporal filter 18 configured to substantially minimize background noise photons in quantum channel 16, such that the signal to noise ratio at receiver 14 is greatly increased.

[0031] Active temporal filter 18 employs an active switching technique to achieve a filter whose gate times represent a substantial improvement compared to electronic filtering techniques. In one example, the active filter comprises gate times in the range of 50fs to 100 ps. Furthermore, the active the active switching technique can result in a substantial improvement in noise tolerance over an electronic filter, and such improvements daytime enable satellite quantum key distribution or quantum communication in bright fibers. In one example, active time filtering achieves an improvement in noise tolerance noise tolerance by a factor of up to 2000 compared to a 2 ns electronic filter. For the sake of comparison, Figure 1b shows a temporal profile and a spectral profile of a noisy signal; Figure 1c shows a temporal profile and a spectral profile of a noisy signal following temporal filtering; and Figure 1d shows a temporal profile and a spectral profile of a noisy signal following active temporal filtering.

[0032] Looking at Figure 1e, there is shown flowchart 100 outlining exemplary steps for implementing active temporal filtering. In one implementation, as shown in Figure 2a, experimental quantum communication system 30 was set up to demonstrate active temporal filtering. Experimental quantum communication system 30 employed a polarization-based decoy state BB84 protocol where noise was intentionally introduced in quantum channel 18 to determine the noise tolerance of quantum communication system 30 using active temporal filter 18. The process starts by generating weak coherent pulses (WCP) prepared by attenuating short pulses at a center wavelength of $\lambda_{\text{signal}} = 720.8 \text{ nm}$, step 102. The weak coherent pulses are obtained from an optical parametric oscillator 32 pumped by titanium-sapphire

(Ti:Sa) laser 33 with a repetition rate of $f_{ref} = 80$ MHz. In step 104, using polarizing beam splitter (PBS) 34 and half-wave plate (HWP) 36, the polarization state of the weak coherent pulses is prepared at Alice's stage or sender 12. According to the standard polarization BB84 protocol, sender 12 randomly prepares the weak coherent pulses in one of four polarization states, i.e. horizontal, vertical, diagonal and anti-diagonal. In step 106, the weak coherent pulses are then attenuated to the single photon level by using neutral density (ND) filter 38 and half-wave plate 36 prior to polarizing beam splitter 34. Next, using half-wave plate 36, the mean photon number of the weak coherent pulses prepared by sender 12 is randomly set to μ , ν , and 0, corresponding respectively to the signal, decoy, and vacuum pulses for the decoy state protocol. The values of μ and ν , are varied for different values of channel noise and loss, and subsequently selected offline to optimize the overall secret key rate for each channel condition.

[0033] In step 108, the weak coherent pulses are then sent through quantum channel 18, where a 10:90 (reflection:transmission) beam splitter 40 is used to introduce channel noise. The noise is produced by second Ti:Sa oscillator 42 operated in continuous-wave mode with a center wavelength and linewidth of $\lambda_{CW} = 720.7$ nm and $\Delta\lambda_{CW} = 0.83$ nm. The amount of noise introduced in channel 18 is controlled using a combination of half-wave plate, polarizing beam splitter and neutral density filter. The polarization of the noise source 42 is randomly varied using an additional half-wave plate. In step 110, the incoming photons are then sent through Bob's detection stage, receiver 14, where the polarization is analyzed using half-wave plate 50 and polarizing beam splitter 52, and then through active temporal filter 18. Using dichroic mirror (DM) 53 and variable delay (VD) stage 54, the signal is made to overlap with a synchronized pump pulse at a center wavelength of $\lambda_{pump} = 800$ nm generated by Ti:Sa oscillator or pump 33, by coupling both into a 10cm-long single mode fibre 58 with coupling efficiencies of 50 % and 65%, for the signal and pump 33 respectively. The switching efficiency, η , of the quantum signal is given by

[0034]

$$\eta = \sin^2(2\theta) \sin^2\left(\frac{\Delta\phi}{2}\right), \quad (1)$$

where θ , is the angle between the polarization of the signal and pump 33, $\Delta\phi = 2\pi n_2 L_{eff} I_{pump} / \lambda_{WCP}$ is the non-linear phase shift induced by the pump single mode fibre 58, n_2 is the nonlinear refractive index of single mode fibre 58, L_{eff} is the effective length of the single mode fiber, and I_{pump} is the intensity of the pump pulse. Maximal switching efficiency is observed when $\theta = \pi/4$ and $\Delta\phi = \pi$. Thus, the polarization of the pump 33 is prepared to be at an angle of 45° to the polarization of the quantum signal at the input of single mode fibre 58. By taking advantage of the difference in group velocity between the quantum signal and the pump pulse inside single mode fibre 58, a uniform nonlinear phase shift is imprinted across the weak coherent pulses. In particular, the pulse duration of pump 33 and the length of single mode fibre 58 is selected to allow the pump pulse to fully traverse through the weak coherent pulses within the length of the single mode fibre 58. This is achieved by spectrally filtering pump 33 with a pair of angle-tuned bandpass filters such that $\Delta\lambda_{pump} = 2:1$ nm. Finally, the average power of the pump pulse is set to 300 mW resulting in a unit switching efficiency.

[0035] Increasing the effective length of medium 58 and the pulse energy of pump 33 may lead to parasitic nonlinear processes such as self-phase modulation and two-photon absorption. These nonlinear processes may create noise photons covering the spectral range of interest for the quantum signals, and therefore the noise photons are appropriately accounted for. In the experimental setup, the unit switching efficiency is achieved by setting the pump pulse energy to 3.75 nJ. At this pulse energy, 1.6×10^{-4} noise counts per pulse originating from pump 33 are detected in the single SST mode dedicated to the quantum signal. Avalanche photo-diode (APD) 60 is then used to detect the measured photons. Avalanche photo-diode 60 is electronically gated using pump 33 as a reference. The coincidence window is dictated by the timing jitter of avalanche photo-diode 60 and was set to $\Delta t_{coinc} = 2.0$ ns. By doing so, a first layer of temporal filtering, or electronic temporal filtering, is achieved by reducing continuous noise by a factor of $f_{rep} \Delta t_{coinc} = 0.16$. Finally, in

step 112, the variable delay stage varying the time of arrival of the pump pulse with respect to the signal is scanned to assess the temporal response of active temporal filter 18, as shown in Figure 2b. The full width at half maximum (FWHM) of the temporal trace is $\Delta t_{\text{switch}} = 0.95 \pm 0.01$ ps with a switching efficiency of $99 \pm 1\%$. To confirm the experimental results, the temporal profile of active temporal filtering was simulated and the simulated results were in substantial agreement with active temporal filter 18 experimental results.

[0036] To assess the feasibility of the time filtering scheme in active quantum communication, a proof-of-principle QKD demonstration was performed, where the figure of merit was given by the secret key rate. In particular, different channel conditions in terms of noise and loss were investigated to demonstrate the different regimes where active quantum communication can offer a considerable advantage over electronic QKD settings. The secret key rate R was calculated using the standard decoy BB84 post-processing procedure, as is known in the art. The following formula was used for key generation:

$$[0037] \quad R \geq q (-Q_{\mu} f(E_{\mu}) H_2(E_{\mu}) + Q_1 [1 - H_2(e_1)]), \quad (2)$$

[0038] where $q = 1/2$ is the sifting efficiency, Q_{μ} is the gain of signal states, $f(x)$ is the error correction efficiency, $H_2(x) = -x \log_2(x) - (1-x) \log_2(1-x)$ is the binary Shannon entropy function, E_{μ} is the quantum bit error rate (QBER), Q_1 is the gain of single-photon states, and e_1 is the error rate of single-photon states. The experimentally measured gains and QBER, i.e. Q_{μ} , Q_{ν} and E_{μ} of optimized mean photon numbers μ and ν for the signal and decoy states, respectively. The standard error correction efficiency factor of $f(E_{\mu}) = 1.22$.

[0039] Experimental results for the secret key rate, R , are shown in Figure 3a comparing the case of electronic temporal filtering and active temporal filtering as a function of channel noise, N , for different values of channel loss. As can be seen, secret key rates can be achieved in a noise regime that is several orders of magnitude larger when operating with active temporal filtering (solid curves) compared to electronic temporal filtering (dashed curves). In particular, the noise threshold, i.e. maximal noise counts that result in a positive secret key rate R , for both temporal

filtering schemes as a function of channel loss is compared, as shown in Figure 3b. The noise threshold is defined as the largest amount of noise for which a positive secret key rate can still be achieved within a standard deviation. The noise tolerance factor, i.e. ratio of noise thresholds for the active temporal filtering to the electronic temporal filtering, is shown in Figure 3c as a function of channel loss, where for certain loss levels, a noise improvement factor in excess of 2000 is obtained, which agrees with the values obtained from the simulation. These results can also be presented in the context of a second scenario where a fixed amount of noise is present in quantum channel 18, but different loss conditions are investigated. The secret key rates are shown as a function of channel loss, as shown Figures 3d and 3e for various noise counts, N . The maximal achievable channel loss can be assessed by considering the loss threshold, see Figure 3f. An improvement in communication distance, i.e. distance improvement factor > 1 occurs for noise counts starting from 1.3×10^3 Hz, see Figure 3g. Moreover, a maximal distance improvement factor is achieved at a channel noise of 8.5×10^4 Hz with an improvement factor of 7. Since, active temporal filter 18 itself introduces small amounts of noise in the measured raw key, benefits are expected particularly in noisy environments. In Figures 3b, f and g, the shaded areas represent conditions where QKD cannot work with an electronic temporal filter, but works with active temporal filter 18. To extend the advantage region of active temporal filter 18, for instance beyond 21 dB of loss, different avenues can be employed to mitigate the effect of pump noise, e.g. pump pulse and SMF engineering. Hence, the reported pump noise is not a fundamental limitation of the active filtering scheme and we expect that lower values of pump noise can be envisaged with further design efforts. Finally, in the experimental setup, the signal wavelength, λ_{signal} , was set to approximately 720 nm. This choice was motivated by the available laser source and the desire for low pump noise, although other wavelengths are also suitable e.g. 1310 nm and 1550 nm. Active temporal filter 18 scheme may be applied to the highly desirable telecommunication wavelengths provided a proper design of single mode fibre 58 and pump 33 either using a polarization rotation switch or other switching schemes. Furthermore, active temporal filter 18 scheme may also improve the noise

tolerance of continuous-variable QKD schemes, where noise and losses are problematic; and also minimizes saturation of the single photon detector.

[0040] When compared to other noise tolerant QKD schemes e.g. for the case of high-dimensional QKD protocol, active temporal filter 18 scheme involving single SST modes has the advantage in noise tolerance when a full high-dimensional analysis of multi-mode quantum signals is carried out compared to a coarse-grained two-dimensional analysis of the multi-mode signal. Furthermore, noise tolerance may be greatly enhanced when the signal is encoded and measured in a single SST mode, noise photons are substantially prevented from even entering the measurement apparatus in modes other than that used to communicate the quantum signals.

[0041] In one exemplary implementation, the transmission of a QKD signal is combined with the transmission of a classical optical signal, such that quantum channels co-exist with classical channels in a quantum communication system.

[0042] In one exemplary implementation, transmitter 12 is a transceiver.

[0043] In one exemplary implementation, receiver 14 is a transceiver.

[0044] It is noted that various example embodiments as described herein may be implemented in a wide variety of devices, network configurations and applications.

[0045] The descriptions of the various embodiments of the present disclosure have been presented for purposes of illustration, but are not intended to be exhaustive or limited to the embodiments disclosed. Many modifications and variations will be apparent to those of ordinary skill in the art without departing from the scope and spirit of the described embodiments. The terminology used herein was chosen to best explain the principles of the embodiments, the practical application or technical improvement over technologies found in the marketplace, or to enable others of ordinary skill in the art to understand the embodiments disclosed herein.

[0046] Embodiments are described above with reference to block diagrams and/or operational illustrations of methods, systems, and computer program products. The operations/acts noted in the blocks may be skipped or occur out of the order as shown in any flow diagram. For example, two or more blocks shown in succession may be executed substantially concurrently or the blocks may sometimes be executed in the

reverse order, depending upon the functionality/acts involved. While the specification includes examples, the disclosure's scope is indicated by the following claims. Furthermore, while the specification has been described in language specific to structural features and/or methodological acts, the claims are not limited to the features or acts described above. Rather, the specific features and acts described above are disclosed as example for embodiments.

CLAIMS:

1. A quantum communication method comprising:
at a sender, preparing photons encoded in a single spatial, spectral, and temporal (SST) mode to form a quantum signal; and introducing the quantum signal into a quantum channel;
at a receiver, a detector and filtering system optically processing the quantum signal and rejecting background noise photons in the quantum channel, and performing active temporal filtering by switching the polarization of the quantum signal without substantially adding noise; and wherein the active temporal filtering minimizes saturation of the detector.
2. The method of claim 1, wherein the detected quantum signal is substantially weaker than the background noise photons, whereby noise tolerance is maximized without significantly altering the quantum signal.
3. The method of claim 2, wherein the photons are prepared for transmission via a fibre network to a receiver.
4. The method of claim 2, wherein the photons are prepared for transmission via a free space channel.
5. The method of any one of claims 1 to 4, wherein the quantum communication protocol comprises quantum key distribution (QKD).
6. The method of claim 1, wherein the active temporal filtering comprises a gate time ranging between 50fs and 100ps.

7. The method of claim 2, wherein the active temporal filter is based on cross-phase modulation via an optical Kerr effect in a single mode fibre.
8. The method of claim 1, wherein the active temporal filter comprises a switching efficiency, η , of the quantum signal, wherein the switching efficiency is dependent on at least the nonlinear refractive index of the single mode fibre and the length of the single mode fibre.
9. The method of claim 1, wherein the active temporal filtering substantially improves the noise tolerance factor and substantially improves the distance compared to electronic filtering techniques.
10. The method of claim 2, wherein the photons are prepared at the sender using a polarizing beam splitter and a half-wave plate according a predetermined polarization protocol.
11. A quantum communication system comprising:
 - a sender comprising a quantum signal source and a quantum signal encoder;
 - a transmission medium;
 - a receiver comprising an active temporal filter and a single photon detector.
12. The quantum communication system of claim 11, wherein the transmission medium is a quantum channel which introduces channel noise.
13. The quantum communication system of claim 12, wherein photons are prepared in a single spatial, spectral, and temporal (SST) mode to form a quantum signal.

14. The quantum communication system of claim 12 or 13, wherein the active temporal filter comprises an active switch of switching efficiency, η , of the quantum signal.
15. The quantum communication system of claim 14, wherein the quantum channel comprises a fibre network.
16. The quantum communication system of claim 15, wherein the switching efficiency is dependent on the nonlinear refractive index of the single mode fibre and the length of the single mode fibre.
17. The quantum communication system of claim 14, wherein the quantum channel comprises free space.
18. An active temporal filter comprising:
a system optically processing a quantum signal and rejecting background noise photons in a quantum channel; operating by
a switch comprising a switching efficiency, η , of the quantum signal, wherein the switching efficiency is dependent on at least the nonlinear refractive index of the single mode fibre and the length of the single mode fibre.
19. The active temporal filter of claim 18, wherein the active temporal filter achieves a substantial improvement in the noise tolerance factor compared to electronic filtering techniques.
20. The active temporal filter of claim 18, wherein the active temporal filter comprises a substantial improvement compared to electronic filtering techniques.

21. The active temporal filter of claim 18, wherein the active temporal filtering comprises a substantial improvement in gate time compared to electronic filtering techniques.

22. The active temporal filter of claim 18, wherein the active temporal filter is based on cross-phase modulation via an optical Kerr effect in a single mode fibre.

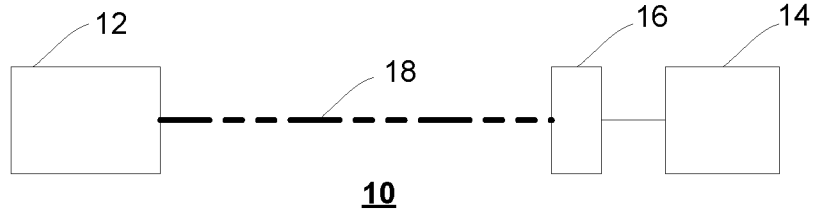


Figure 1a

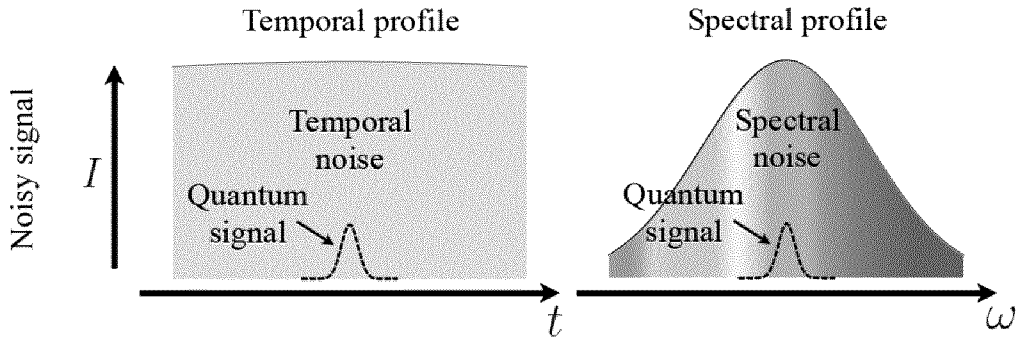


Figure 1b

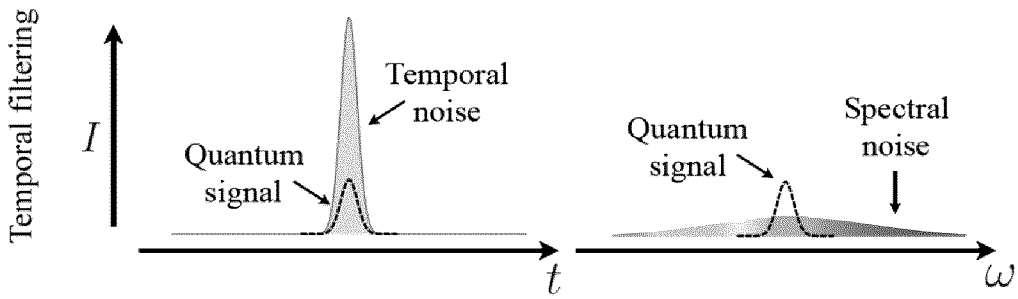


Figure 1c

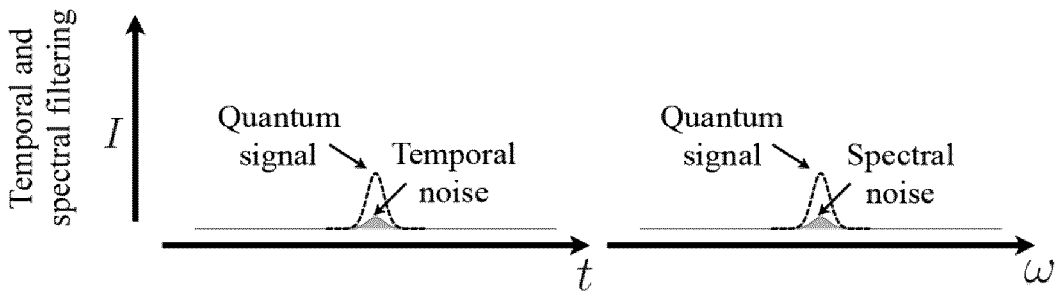


Figure 1d

2/5

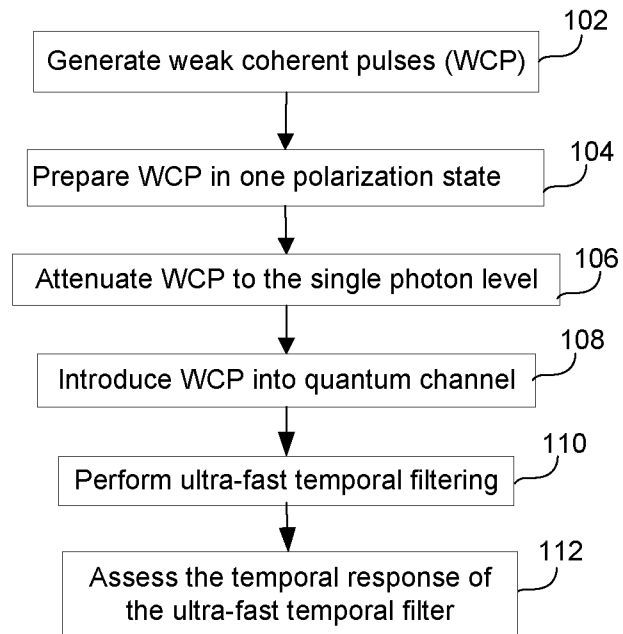
**100**

Figure 1e

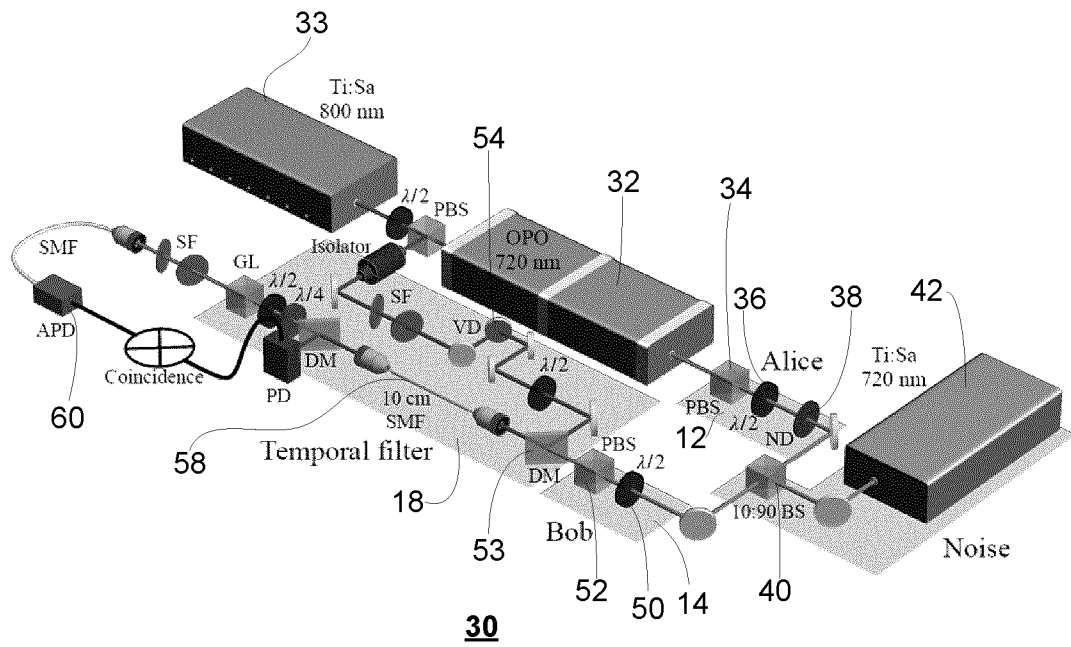


Figure 2a

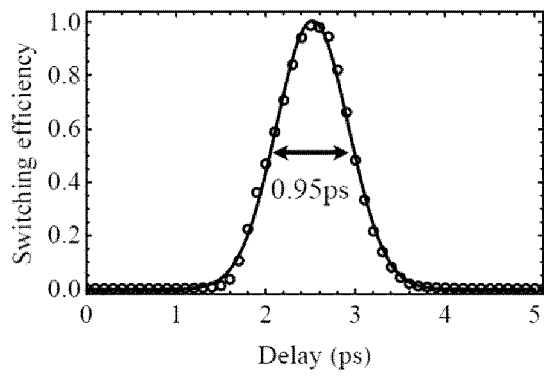


Figure 2b

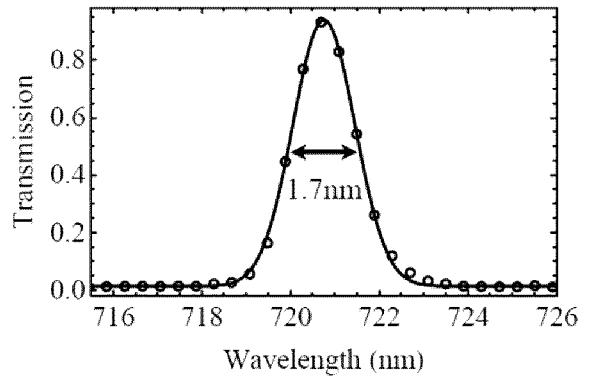


Figure 2c

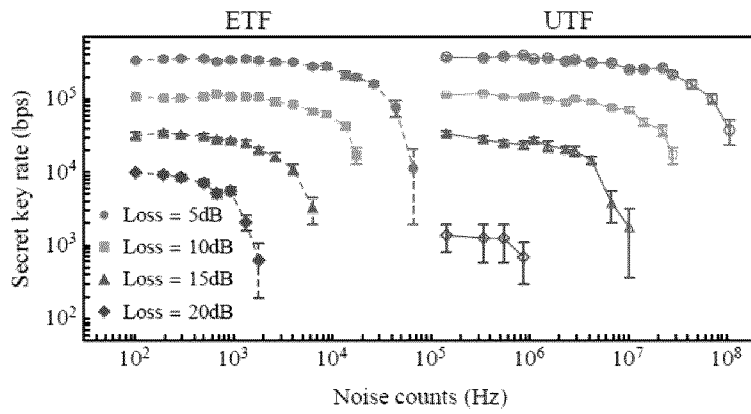


Figure 3a

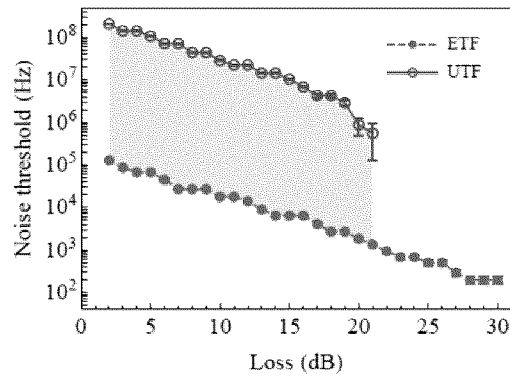


Figure 3b

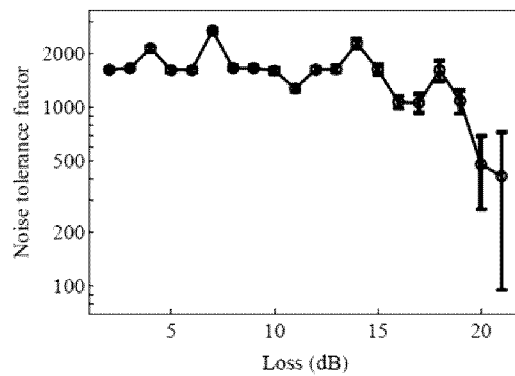


Figure 3c

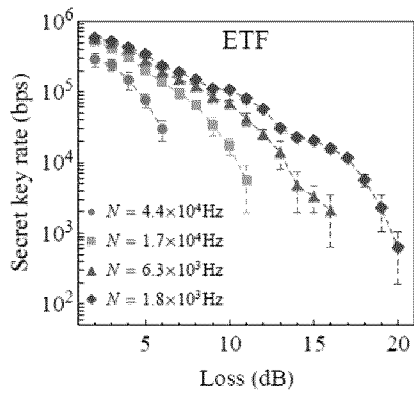


Figure 3d

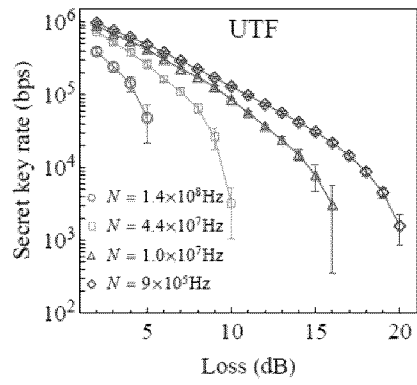


Figure 3e

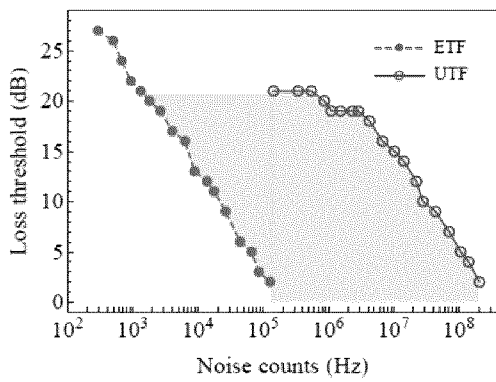


Figure 3f

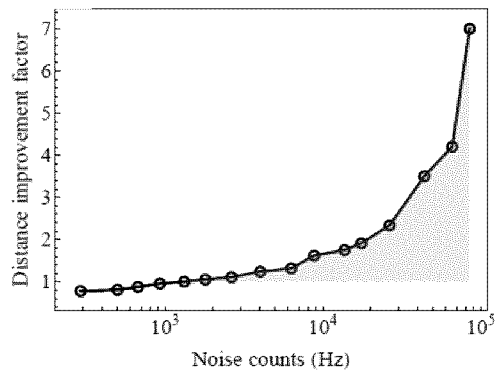


Figure 3g

INTERNATIONAL SEARCH REPORT

International application No.

PCT/CA2021/050686

A. CLASSIFICATION OF SUBJECT MATTER

IPC: **H04B 10/70** (2013.01), **B82Y 20/00** (2011.01), **G02B 27/09** (2006.01), **G02B 27/28** (2006.01),
G02F 1/035 (2006.01), **H04B 10/25** (2013.01) (more IPCs on the last page)

According to International Patent Classification (IPC) or to both national classification and IPC

B. FIELDS SEARCHED

Minimum documentation searched (classification system followed by classification symbols)

IPC: **H04B 10/70** (2013.01), **B82Y 20/00** (2011.01), **G02B 27/09** (2006.01), **G02B 27/28** (2006.01),
G02F 1/035 (2006.01), **H04B 10/25** (2013.01), **H04B 10/60** (2013.01), **H04B 10/60** (2013.01)

Documentation searched other than minimum documentation to the extent that such documents are included in the fields searched

Electronic database(s) consulted during the international search (name of database(s) and, where practicable, search terms used)

Database: (Orbit: Keywords: quantum communication, single, spatial, spectral, temporal, SST, quantum signal, background noise, active temporal filtering, active temporal filter, saturation, detector, optical, qkd, switch, switching efficiency, gate, kerr, refractive index)

C. DOCUMENTS CONSIDERED TO BE RELEVANT

Category*	Citation of document, with indication, where appropriate, of the relevant passages	Relevant to claim No.
X	US 2019/0379463 A1 (SHIELDS et al.) 12 December 2019 (12-12-2019) (see whole document)	11
A	US 9,036,817 B1 (Hunt et al.) 19 May 2015 (19-05-2015) (see whole document)	1-10, 12-22
A	US 2015/0372768 A1 (DYNES et al.) 24 December 2015 (24-12-2015) (see whole document)	1-10, 12-22

Further documents are listed in the continuation of Box C.

See patent family annex.

* Special categories of cited documents:	“T” later document published after the international filing date or priority date and not in conflict with the application but cited to understand the principle or theory underlying the invention
“A” document defining the general state of the art which is not considered to be of particular relevance	“X” document of particular relevance; the claimed invention cannot be considered novel or cannot be considered to involve an inventive step when the document is taken alone
“D” document cited by the applicant in the international application	“Y” document of particular relevance; the claimed invention cannot be considered to involve an inventive step when the document is combined with one or more other such documents, such combination being obvious to a person skilled in the art
“E” earlier application or patent but published on or after the international filing date	“&” document member of the same patent family
“L” document which may throw doubts on priority claim(s) or which is cited to establish the publication date of another citation or other special reason (as specified)	
“O” document referring to an oral disclosure, use, exhibition or other means	
“P” document published prior to the international filing date but later than the priority date claimed	

Date of the actual completion of the international search
05 July 2021 (05-07-2021)

Date of mailing of the international search report
05 August 2021 (05-08-2021)

Name and mailing address of the ISA/CA
Canadian Intellectual Property Office
Place du Portage I, C114 - 1st Floor, Box PCT
50 Victoria Street
Gatineau, Quebec K1A 0C9
Facsimile No.: 819-953-2476

Authorized officer

Camran Syed (819) 635-5801

INTERNATIONAL SEARCH REPORT
Information on patent family members

International application No.
PCT/CA2021/050686

Patent Document Cited in Search Report	Publication Date	Patent Family Member(s)	Publication Date
US2019379463A1	12 December 2019 (12-12-2019)	US2019379463A1 GB201809496D0 GB2574597A JP2019216413A JP6852115B2	12 December 2019 (12-12-2019) 25 July 2018 (25-07-2018) 18 December 2019 (18-12-2019) 19 December 2019 (19-12-2019) 31 March 2021 (31-03-2021)
US 9,036,817 B1	19 May 2015 (19-05-2015)	None	
US2015372768A1	24 December 2015 (24-12-2015)	US2015372768A1 US9634770B2 GB201411114D0 GB2534109A GB2534109B GB201704283D0 GB2550263A GB201704285D0 GB2550264A GB2550264A9 GB2550264B JP2016010161A JP6007291B2	24 December 2015 (24-12-2015) 25 April 2017 (25-04-2017) 06 August 2014 (06-08-2014) 20 July 2016 (20-07-2016) 26 September 2018 (26-09-2018) 03 May 2017 (03-05-2017) 15 November 2017 (15-11-2017) 03 May 2017 (03-05-2017) 15 November 2017 (15-11-2017) 25 July 2018 (25-07-2018) 26 September 2018 (26-09-2018) 18 January 2016 (18-01-2016) 12 October 2016 (12-10-2016)